

PAPER • OPEN ACCESS

Geometrical and mechanical performance of multi-material fused deposition modelling

To cite this article: N A Alief *et al* 2019 *IOP Conf. Ser.: Mater. Sci. Eng.* **557** 012022

View the [article online](#) for updates and enhancements.

Geometrical and mechanical performance of multi-material fused deposition modelling

N A Alief¹, M S Utomo², I Kartika², and Y Whulanza^{1,3}

¹ Department of Mechanical Engineering, Universitas Indonesia

² Research Center for Metallurgy and Materials, Indonesia Institute of Sciences

³ Research Center for Biomedical Engineering, Universitas Indonesia

Abstract. One method that has been used on additive manufacturing process is fused deposition modelling (FDM). This method employs material extrusion in the form of filament to build a product. Several materials have been developed as the filament, each with its own mechanical, chemical, and thermal properties. Certain FDM machines are capable to print filaments from different materials. Although, each materials require different printing parameters. Consequently, different geometrical and mechanical properties from same design may be produced from their different printing parameters. Therefore, in order to obtain the characteristic of FDM machine output on multi-material, a comparative study is conducted. Lattice structures constructed from 3D CAD model with difference in pore configuration are printed by different filament materials on same FDM machine. We investigate the geometrical and mechanical properties of the structure, especially on the capability of the lattice structure to bear compressive load. There are 42-53% of pore dimension difference between the printed structure and the design despite material variation is used for each pore configuration.

1. Introduction

Fused Deposition Modelling (FDM) is currently become a popular fabrication process and commonly used for modelling, prototyping, and production application [1]. This process favour the ease of fabricating three-dimensional objects of almost any form and less waste than traditional subtractive production method [2]. As one of methods in additive manufacturing process, fused deposition modelling utilizes extrusion of material formed in filament to build structural 3D model by layering from bottom to the top. The filament is melted according to the melting temperature of certain material and extrusion occurs through the nozzle, subsequently. Materials are subjected to phase changes under relatively high temperature [3]. The material is soon after being deposited and it cools down and solidifies right after deposition [4]. The movement of the nozzle is based on the process parameters resulting the path generation. A desired structure, such as accurate dimension and splendid mechanical performance, may be achieved accurately and precisely by configuring each component of parameters.

Wide range materials, from polymers, ceramics, to metals [5], has been developed into 3D printing filaments. These materials have two main roles, which could be as the build material and support material [1]. The common material combination is Polylactic Acid (PLA) and Polyvinyl Alcohol (PVA). Besides that PLA is the most widely used material in extrusion-based 3D printing technique



Content from this work may be used under the terms of the [Creative Commons Attribution 3.0 licence](https://creativecommons.org/licenses/by/3.0/). Any further distribution of this work must maintain attribution to the author(s) and the title of the work, journal citation and DOI.

[6] is easy to print and biodegradable [7]. On the other hands, PVA generally takes a role as the support material due to the ease of removal from the built structure. Both of them has intersect melting temperature value, PLA has 150-220°C [8-11] and PVA has melting temperature range of 190–220°C [12]. Therefore, this combination has been utilized in order to build three-dimensional structure.

Several comparative studies has been conducted on the FDM scope. Ceretti, et.al. [3] conducted a comparison between grain and wire FDM process. Minetola et.al. [4] presented the benchmarking analysis of Prusa i3 machine improvements. Loh, et.al [13] compared FDM with other rapid prototyping techniques. Gregor, et. al. [14] attempted to overcome technical limitations and fabricate scaffolds using current, cheap and commercially available devices and materials. Zein et.al. [15] compared the 3d printed results that have various combination of pattern. Tagami 2018 [16] conduct studies between FDM printed PLA and PVA for preparation of multi-component tablets. The characteristic of the FDM output differs due to the material variation. Therefore, a comparative study between PLA and PVA-made lattice structure with two types of pore configuration is conducted.

2. Methods

2.1. Designing the Lattice Structure

Lattice structure formed with two types of pore configuration.in cube. One has pore dimension of 1000 μm and the other one has 1500 μm length, as shown on the Figure 1. Both has uniform length and width of 12.5 mm yet each of the configuration has different height. The 1000 microns has 14mm and the other one has 15mm. The pore itself has identical square shape. Each configuration is printed with two types of material, which are PLA and PVA.

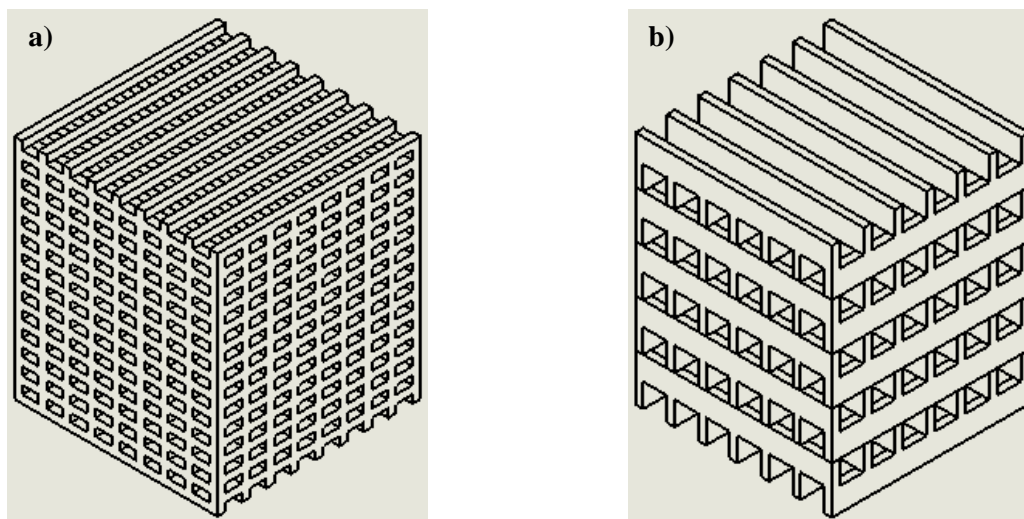


Figure 1. Lattice Structure Design with two types of configuration. a) 1000 μm length b) 1500 μm length.

2.2. Printing Setup

Before structures are fabricated, CAD models are saved on triangulated form as .stl file format. Each structure with different pore configuration are then being input to the built-in slicer software of the FDM machine. On the software, the lattice is replicated into four pieces in order to print in one batch. Afterwards, we set the material, building orientation, and process parameters. Standard mode, one of three printing options, is chosen within particular quantity of each component as seen on Table 1.

Once the process parameters are set, the nozzle path can be generated and results on .gsd file format and building estimation for each batch. The study is conducted by building two batches for each material and pore configuration.

Table 1. Amount of each process parameter for the standard printing mode.

Parameter settings	Value
Print Speed (mm/s)	60
Extrude Speed (mm/min)	45
Nozzle Temperature (°C)	195
Layer Thickness (mm)	0.1
Number of Solid Surface Layer	4
Number of Solid Shell Layer	1
Infill Line Distance (mm)	5
Strip Rate	2.6
Support Angle	50

2.3. Characterization

2.3.1. Pore Dimension Measurement. Two lattice structures are taken as the sample from each batch of material and pore configuration, thus there are 16 pieces of lattice structure sample. The samples are then being captured by calibrated digital microscope which has measurement feature on the axial view. Each pore sample from the chosen lattice structure is measured with designated arrangement. The lattice dimension is also measured as the same view as pore measurement.

2.3.2. Compressive Load Test Setup. Three samples of each pore dimension and material combination were subjected to compressive load test. Since there were two material and two pore dimensions, there were twelve samples in total. Compressive load test was conducted on Shimadzu AG-50kN XPlus. The room temperature and humidity during testing were 21.5 °C and 52.3 % respectively. Each sample was subjected to tensile rate of 10 mm/min.

3. Result and Discussion

3.1. Geometrical Performance

Based on the lattice formation, both the 1000 microns and 1500 microns have consistent square-shaped pore on the center part of lattice. Besides, the pore formation on the peripheral region has not complied the desired model yet each of the pore on this location is much alike one on another. In addition, it is observed that each corner of the lattice formed a round corner due to the cylindrical form of melted filament. The comparison of lattice formation between PLA and PVA material can be seen on the Figure 2. In contrast to the PLA lattice, PVA structure tend to have more fibrous filaments that is trapped inside the structure which need micro equipment for cleaning the fibers.

The measurement of overall lattice formation has been obtained. It is resulted in area and height of lattice structure. The 1000 microns has the average area of 155.74 mm² (standard deviation of sample [SD_{sample}] = 0.97) and 13.8 mm (SD_{sample} = 0.11) height whereas the other pore configuration has 154.07 mm² (SD_{sample} = 1.31) of the average pore area and height of 14.63 mm (SD_{sample} = 0.17). The measurement also resulted in area of each pore sample. According to the pore configurations, it is

obtained that the average pore area is 0.497 mm^2 with standard deviation of 0.08 for 1000 microns and 0.952 mm^2 with standard deviation of 0.16 for 1500 microns. However, from the Figure 3, the lattice structures from both material has relative change with respect to the preliminary design in a range of 42% to 53%. Thus, these reveal that the layer thickness has an influence towards the proportion of printed structure. According to the machine specification, this machine has 0.4 nozzle diameter. Hence, in order to obtain the value of layer thickness, the melted filament is urged to the sides of the nozzle. This causes a reduction on the pore dimension.

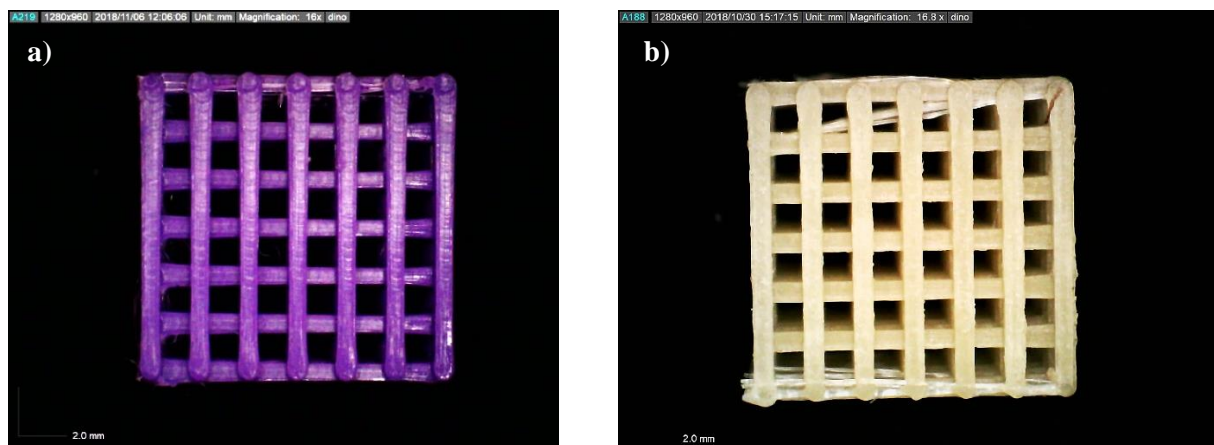


Figure 2. Samples of 1500 microns lattice structures with different filament materials. a) Polylactic Acid (PLA). b) Polyvinyl Alcohol (PVA).

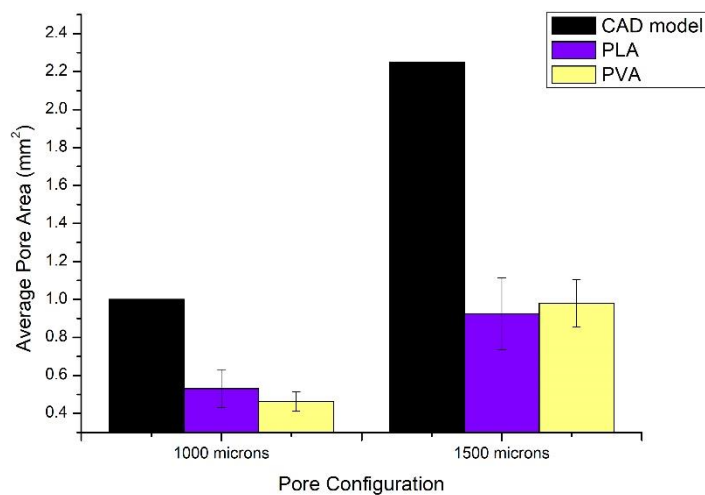


Figure 3. Graph of pore dimension for each pore configuration and materials.

The uniformity among pores on the central part and peripheral region is also being examined. Based on Figure 4, uniformity is occurred on each observed region regardless the material and the pore configuration. Thus, the machine can fabricate lattice precisely.

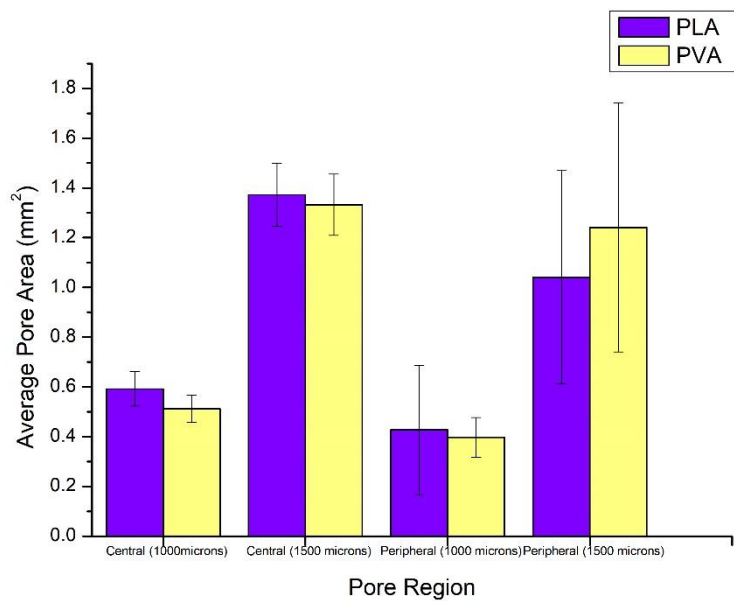


Figure 4. Average area in central and peripheral region for both pore configuration and materials.

3.2. Mechanical Performance

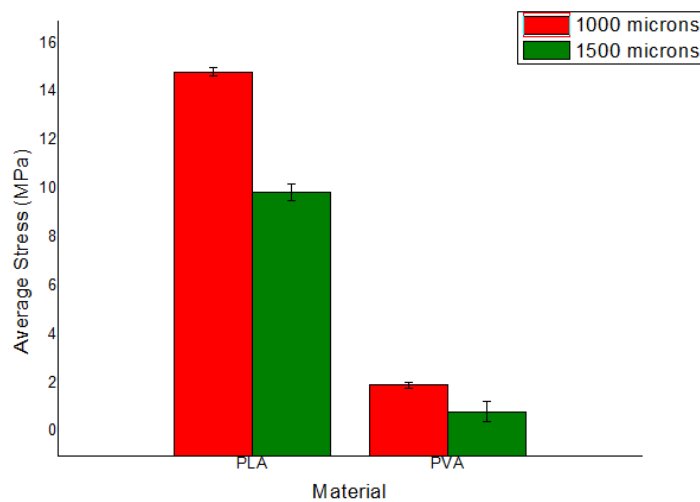


Figure 5. Graph of compressive load for each pore configuration and materials.

Figure 5 shows the result of compressive load test. At a glance, lattice structures made from PLA exhibit higher capability to withstand compressive load compared to lattice structures made from PVA for both pore configurations. Lattice structures made from PLA show average compressive strength of 9.87 and 14.84 MPa for pore dimension of 1500 and 1000 microns respectively. Meanwhile, lattice structures made from PVA show average compressive strength of 0.83 and 1.96 MPa for pore dimension of 1500 and 1000 microns respectively.

It can be seen from the result that both material and pore dimension affect mechanical properties of the 3D-printed polymeric lattice structures. For lattices with pore dimension of 1500 microns,

compressive strength ratio between PLA and PVA is 12:1. Meanwhile, for lattices with pore dimension of 1000 microns, compressive strength ratio between PLA and PVA is 7.6:1.

The ratio of compressive strength on pore dimension between samples made from PLA show that samples with 1500 microns has compressive strength 0.67 times lower than samples with 1000 microns. Meanwhile, the ratio of compressive strength on pore dimension between samples made from PVA show that samples with 1500 microns has compressive strength 0.43 times lower than samples with 1000 microns.

4. Conclusion

Geometrical evaluation of 3D-printed polymeric lattice structures by optical measurement show that using current combination of printing machine, filament material, and printing parameters, the realized products deviated 40 to 50 % from the desired model. This result should be put into consideration when 3D-printed materials are required to have precise dimension in application. Optimization is needed in order to achieve more accurate result on geometrical and mechanical performance of lattice structure. Compressive load test shows that combination of pore geometry and materials can be utilized to produce lattice structures with specific mechanical strength. This could be further characterized and utilized for specific usage.

Acknowledgments

This research is funded by 2018 Insinas grant scheme from Indonesian Ministry of Research and Higher Education. Authors would like to thank colleagues and technical staff for their technical and non-technical support.

References

- [1] Mohamed O A, Masood S H, and Bhowmik J L 2015 *Adv. Manuf.* **3**(1) 42-53
- [2] Ramos-Lozano S, Molina-Salazar J, Rico-Pérez L, and Atayde-Campos D 2019 *Best Practices in Manufacturing Processes* (Cham: Springer) p 389-410
- [3] Ceretti E, Ginestra P, Neto P I, Fiorentino A, and Da Silva J V L 2017 *Procedia CIRP* **65** 13-18
- [4] Minetola P, Galati M, Iuliano L, Atzeni E, and Salmi A 2018 *Procedia CIRP* **67** 203-208
- [5] Do A-V, Khorsand B, Geary S M, and Salem A K 2015 *Adv. Healthc. Mater.* **4**(12) 1742-1762
- [6] Lopes L R, Silva A F, and Carneiro O S 2018 *Addit. Manuf.* **23** 45-52
- [7] Bagaria V, Bhansali R, Pawar P 2018 *J. Clin. Orthop. Trauma.* **9**(3) 207-212
- [8] Castro-Aguirre E, Iñiguez-Franco F, Samsudin H, Fang X, and Auras R 2016 *Adv. Drug. Deliv. Rev.* **107** 333-366
- [9] Martin O and Avérous L 2001 *Polymer* **42** (14) 6209-6219
- [10] Jing X, Mi H Y, Peng X F, and Turng L S 2015 *Polym. Eng. Sci.* **55** (1) 70-80
- [11] Leist S K, Gao D, Chiou R, and Zhou J 2017 *Virtual. Phys. Prototyp.* **12**(4) 290-300
- [12] Goyanes A, Kobayashi M, Martínez-Pacheco R, Gaisford S, and Basit A W 2016 *Int. J. Pharm.* **514**(1) 290-295
- [13] Loh Q L and Choong C 2013 *Tissue. Eng. Part. B. Rev.* **19**(6) 485-502
- [14] Gregor A, Filová E, Novák M, Kronek J, Chlup H, Buzgo M, Blahnová V, Lukášová V, Bartoš M, Nečas A and Hošek J 2017 *J. Biol. Eng.* **11**(1) 31
- [15] Zein I, Hutmacher D W, Tan K C, and Teoh S H 2005 *Biomaterials* **23**(4) 1169-1185
- [16] Tagami T, Nagata N, Hayashi N, Ogawa E, Fukushima K, Sakai N, and Ozeki T 2018 *Int. J. Pharm* **43**(1-2) 361-367